

1 **Aerosol-rainfall relationship over the Middle East and North Africa (MENA) region from**  
2 **observations**

3

4 Sagar P. Parajuli<sup>1\*</sup>

5

6

7 <sup>1</sup>King Abdullah University of Science and Technology, Thuwal, Saudi Arabia

8

9

10

11

12

13

14 \*Corresponding Author, E-mail: [psagar@utexas.edu](mailto:psagar@utexas.edu)

15

16 This is not a peer-reviewed research article. It is a preprint submitted to EarthArXiv. This article  
17 is not under consideration in any other journals.

18 **Abstract**

19 Water is an essential element of life and rainfall. The amount of rainfall directly affects the  
20 spatial and temporal distribution of water resources on the Earth. Rainfall has direct impact on  
21 agricultural production, daily life activities, and human health. Atmospheric aerosols are  
22 essential for rainfall formation; therefore, understanding how dust compositions and distributions  
23 affect the regional rainfall pattern is of utmost importance, particularly in the region with high  
24 atmospheric dust loading, such as the Middle East and North Africa (MENA). Although aerosol-  
25 rainfall research has gained increased attention in the last few decades, many details of aerosol-  
26 cloud-rainfall interactions pathways remain unknown. In this work, dust-rainfall connection is  
27 examined using a large sample of Aerosol Optical Depth (AOD) and rainfall data from Moderate  
28 Resolution Imaging Spectroradiometer (MODIS) and Tropical Rainfall Measuring Mission  
29 (TRMM), respectively, obtained on daily basis for the years 2015 and 2016 over the MENA  
30 region. Observational analysis reveal that rainfall is oppositely related to AOD in low and high  
31 rainfall conditions. Exponentially decreasing (increasing) relationship with AOD under low  
32 (high) rainfall conditions, at a similar range of AOD in both cases, was observed. Further  
33 analysis using angstrom exponent data suggest that the positive (negative) relationship between  
34 AOD and rainfall could represent dust indirect effects during the mature (initial) stage of  
35 convection. This observational analysis provide a basis to predict rainfall under different dust  
36 loading conditions (AOD) using satellite data and provide a benchmark for improving the  
37 representation of dust effect on cloud and rainfall processes in the models, which currently have  
38 significant uncertainty. While dust and dust storms are considered nuances from air quality  
39 perspective, these results highlight their fundamental positive impact on Earth's climate.

40

## 41 1. Introduction

42

43 Tiny aerosol particles floating in the atmosphere have several implications on the Earth's climate  
44 and its inhabitants. When they are concentrated near the surface, they pose threat to the human  
45 and animal health by degrading the air quality (Parajuli et al., 2019; Ukhov et al., 2020). Since  
46 they can scatter solar radiation back to space and absorb radiation within the aerosol layers, they  
47 can also affect the atmospheric circulations by causing heat imbalance on the surface of Earth  
48 and its atmosphere (e.g., Sokolik and Toon, 1996; Jacobson et al., 2006; Kalenderski and  
49 Stenchikov, 2016). They are also known to affect the rainfall patterns through various direct and  
50 indirect pathways (e.g., Lohmann and Feichter, 2001; Abbott and Cronin, 2021; Koren et al.,  
51 2005). Since the entire biosphere including human beings directly depend upon rainfall for their  
52 survival, changes in rainfall patterns can have broader, and long-term consequences. Unequal  
53 distribution of rainfall can affect the frequency and intensity of floods and droughts and affect  
54 the distribution of regional water resources. Changes in prevailing monsoon system and rainfall  
55 pattern can affect agricultural production, limit access to drinking water supply, and affect daily  
56 life activities. Therefore, understanding how the atmospheric aerosol in a region affects the  
57 regional rainfall pattern is of great concern.

58 Due to multiple feedbacks of aerosols on Earth's climate that occur through various direct and  
59 indirect pathways, it is not easy to understand their effect on rainfall. Dust can both increase and  
60 decrease rainfall by affecting local circulations through their direct effect (Jacobson et al., 2006;  
61 Rémy et al., 2015). For example, in West Africa, dust can reduce rainfall by inducing a cooling  
62 effect that decreases the meridional gradient of moist static energy (Konare et al., 2008). In  
63 contrast, dust can also enhance rainfall through dust-induced diabatic warming in the higher  
64 troposphere that enhances regional circulation (Jin et al., 2015) through the elevated heat pump  
65 effect (Lau et al., 2010).

66 Dust can also affect rainfall by directly altering the process of condensation. Only a fraction of  
67 all aerosol particles available in the atmosphere can nucleate or condense on the surface of  
68 atmospheric particles to form cloud droplets; these particles are called cloud condensation nuclei  
69 (CCN) (Stull, 2000; Dennis, 1980). Homogenous and heterogeneous nucleation are the  
70 nucleation that happens in the absence and presence of hydrophilic aerosol particles, respectively  
71 (Stull, 2000). The number density of CCN activated increases with the increase in  
72 supersaturation (Stull, 2000). Similarly, ice nuclei (IN) are specific atmospheric particles such as  
73 bacteria and dust, which promote the freezing of supercooled cloud droplets and produce ice  
74 crystals (Creamean et al., 2013). The mixed-phase cloud so produced initiates precipitation  
75 which is much more faster than supercooled, liquid-only cloud because of the faster growth rate  
76 of ice particles versus droplets (Pinsky et al., 1998). Ice crystals nucleate through different  
77 processes including homogeneous freezing, heterogeneous freezing, immersion freezing, contact  
78 freezing, and condensation freezing. These principles of indirect effects of aerosols on rainfall  
79 are mainly founded on the pioneering experimental works of Coulier (Coulier, 1875) and Aitken  
80 (Aitken, 1882), who showed the ability of tiny dust/aerosol particles to form clouds or fogs in a  
81 simple device (Verzár, 1959). Dust can act both as IN (Creamean et al., 2013), which mainly

82 affect the cold cloud processes (Ansmann et al., 2005) and CCN, which mainly affects warm  
83 cloud processes (Li et al., 2010; Twohy, 2015).

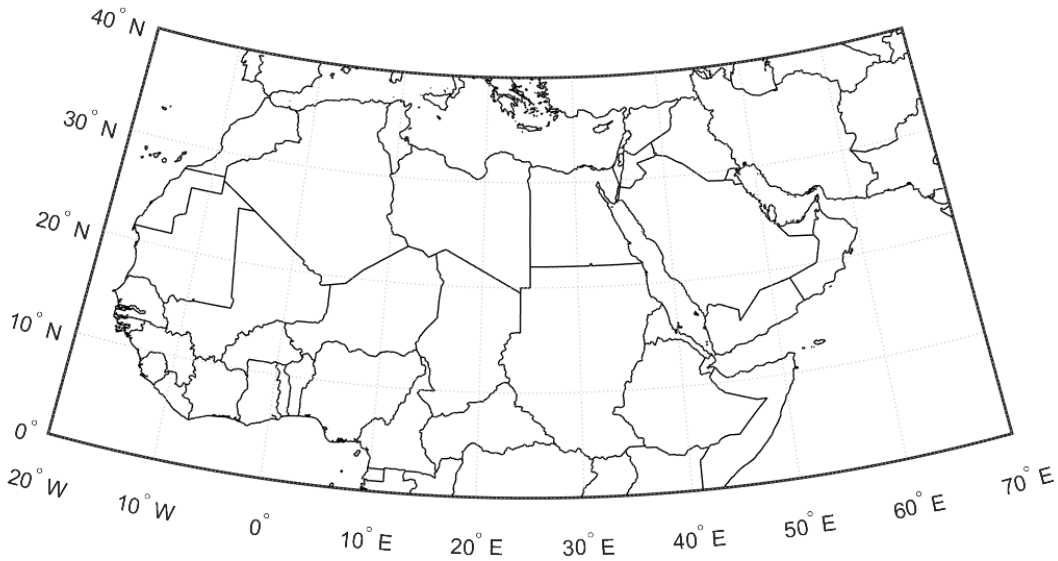
84 A recent modeling study (e.g., Alizadeh-Choobari, 2018) has shown that aerosols increase  
85 rainfall during heavy rainfall events and suppress light rainfall events. Through observations, Li  
86 et al. (2011) found that aerosols increase (decrease) rainfall in clouds with high (low) liquid  
87 water content. Han et al. (2009) also showed show strong negative correlation between  
88 atmospheric dust loading and rainfall over the dust source regions of the Tibetan Plateau using  
89 observations. Although multiple new mechanisms have been proposed recently to explain the  
90 underlying causes of the increasing and decreasing effect of aerosols on rainfall (e.g., Fan et al.  
91 2018; Grabowski and Morrison, 2020; Abott and Cronin, 2021), they are still debated and at  
92 times controversial (Alizadeh-Choobari, 2018) despite extensive research interest on the topic.  
93 Although the opposite effects of aerosols on light and heavy rainfall is well known, the exact  
94 relationship between aerosol loading and rainfall has not been found. In this context, there is a  
95 need to reexamine the dust-rainfall connections from a new perspective. Therefore, in this work,  
96 the effect of dust on rainfall over the MENA region is analyzed with an aim to answer the  
97 following particular research questions.

- 98 1. How is atmospheric aerosol loading related to rainfall?
- 99 2. Is there any physically based relationship between rainfall and AOD found in  
100 observations?

## 101 **2. Data and Methods**

### 102 **2.1. Study domain and data**

103 To understand dust-rainfall connections from observations, a diverse and comprehensive sample  
104 is created to include a range of dust and rainfall data observed in reality. For this observational  
105 study, the analysis is focused over the entire MENA region (-20 to 70E and 0 to 40N), outlined  
106 by the outermost box in Fig. 1 (d01). The area covers the Sahel region including some part of the  
107 African rain forest in the south and the northern regions that experience frequent dust storms, so  
108 a large range of possible rainfall and AOD values lie within the domain.



109

110 Figure 1. The study region showing the MENA region used for observational analysis.

111 Precipitation data from Tropical Rainfall Measurement Mission (TRMM) (Liu et al., 2012) is  
 112 used in this study. The 3B42 daily-accumulated precipitation data (TRMM\_3B42\_Daily)  
 113 available at  $0.25^\circ \times 0.25^\circ$  resolution, which are generated from the research-quality 3-hourly  
 114 TRMM Multi-Satellite Precipitation Analysis TMPA (3B42). Further details of the rainfall  
 115 retrieval algorithm can be found in Huffman et al. (2016).

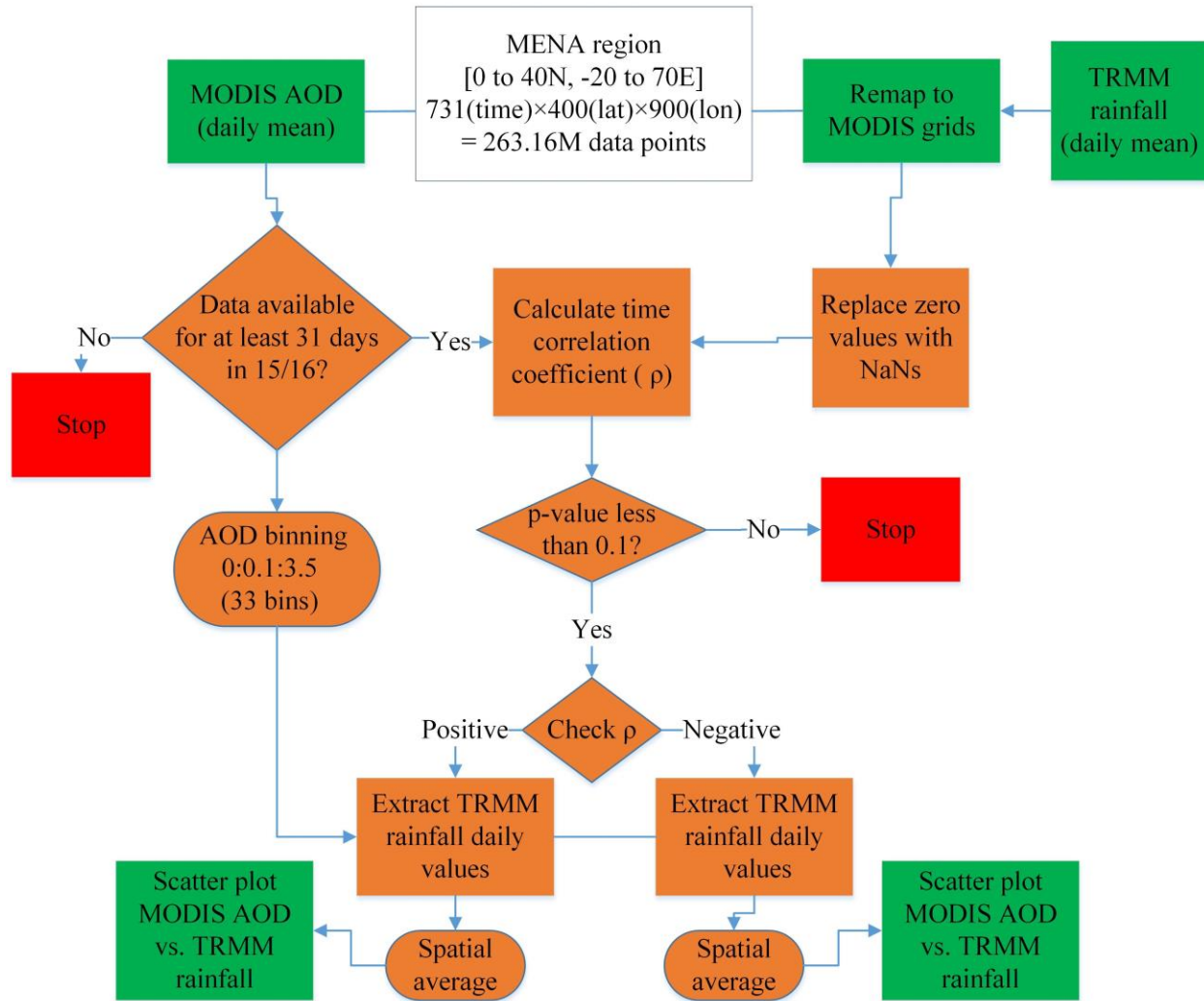
116 For aerosols, Moderate Resolution Imaging Spectroradiometer (MODIS) level-2 Deep Blue  
 117 AOD data (MYD04\_L2 and MOD04\_L2) at 550 nm (Hsu et al., 2004) are used, which are  
 118 available daily, for the whole globe, at a resolution of  $\sim 0.1^\circ \times 0.1^\circ$ . The MODIS AOD collection  
 119 6 dataset is used which has an enhanced Deep Blue aerosol retrieval algorithm (Hsu et al., 2013).  
 120 Although a newer version (collection 6.1) is available (Sayer et al., 2019), we continue to use  
 121 collection 6 because we did not notice remarkable difference in the spatial pattern of AOD  
 122 between these two versions. We use the data with quality flag 1 (QF = 1). Although higher QF (2  
 123 or 3) is recommended for general use (Sayer et al., 2013), we use QF = 1 because using higher  
 124 QFs reduces the number of samples considerably and there is no much added benefit of using  
 125 higher-resolution, level-2 data compared to coarser-resolution, level-3 data when QF = 3 is used.  
 126 The average of daily AOD from Terra and Aqua satellites is used for analysis, which represent  
 127 measurements at  $\sim 10:30$  a.m. and  $\sim 1:30$  p.m. local time, respectively. We also use Angstrom  
 128 Exponent (AE) at 470/660 nm from the same MODIS dataset. The AE is related to the size of  
 129 dust particles because AE greater (smaller) than 0.75 typically represents fine-mode (coarse-  
 130 mode) dust, respectively (Eck et al., 1999; Parajuli et al., 2017).

131 We also use the divergence  $(\frac{\partial u}{\partial x} + \frac{\partial v}{\partial y})$  data from European Centre for Medium-Range Weather  
 132 Forecasts (ECMWF) operational analysis in this study. The horizontal divergence of the velocity  
 133 field is related to the vertical motion with positive (negative) values indicating downward  
 134 (upward) motion caused by diverging (converging) airflow.

135

### 136 **2.3. Methods**

137 The daily MODIS AOD and TRMM rainfall data over the MENA region (Fig. 1, d01) for the  
138 two entire years 2015 and 2016 are used. To extract the relationship between AOD and rainfall,  
139 an inverse approach is adopted as described below. In the first step, the TRMM rainfall data  
140 ( $0.25^\circ \times 0.25^\circ$ ) is remapped to the MODIS grid resolution ( $0.1^\circ \times 0.1^\circ$ ) using a first-order mass-  
141 conserving remapping technique, which is the preferred approach for rainfall data, as opposed to  
142 other commonly used interpolation techniques. Reprojection results in 731 (time) x 400 (lat) x 900  
143 (lon) grid cells, consisting of more than 263 million potential data points. Note that MODIS data  
144 contains many NaNs in the data because of cloud cover and other algorithm constraints so the  
145 actual data used for analysis are much less. As a quality control measure, only those grid cells  
146 that have at least 31 days of AOD data in the years 2015/16 are used. For consistency, since  
147 TRMM reports zero values when there is no precipitation, zero values are also replaced with  
148 NaNs in the TRMM dataset so that the statistical calculations are not biased. In the second step,  
149 the temporal correlations between AOD and rainfall are calculated in each grid cells. In  
150 subsequent analysis, the grid cells that shows p-value  $> 0.1$  are masked out, to ensure that all the  
151 correlations calculated have more than 90% confidence level. In the third step, all daily-mean  
152 AOD values for 2015/16 over the MENA region were grouped into 33 different bins (0:0.1:3.25)  
153 and TRMM rainfall was extracted corresponding to those bins, separately for grid cells showing  
154 positive and negative correlations. The extracted rainfall data was then averaged spatially over  
155 all grid cells with the given sign of the correlation and plotted against the AOD data, resulting in  
156 two comparisons. The above process is summarized in the flow chart presented in Fig. 2.



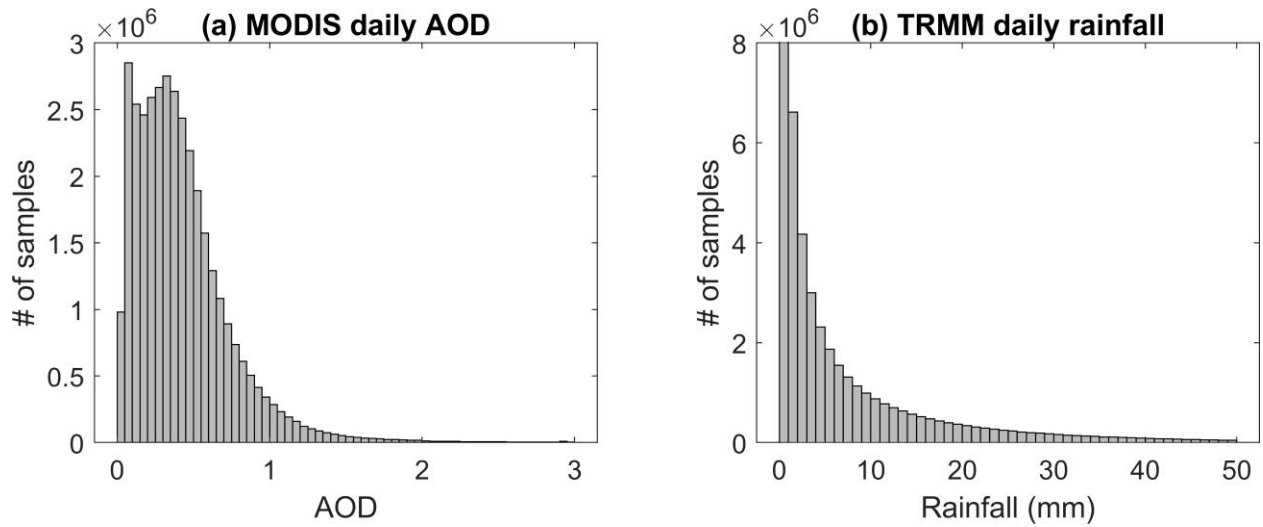
157

158 Figure 2. Flow chart showing the data processing steps and analysis procedure adopted to  
 159 understand dust-rainfall connection from observations.

160 **3. Results**

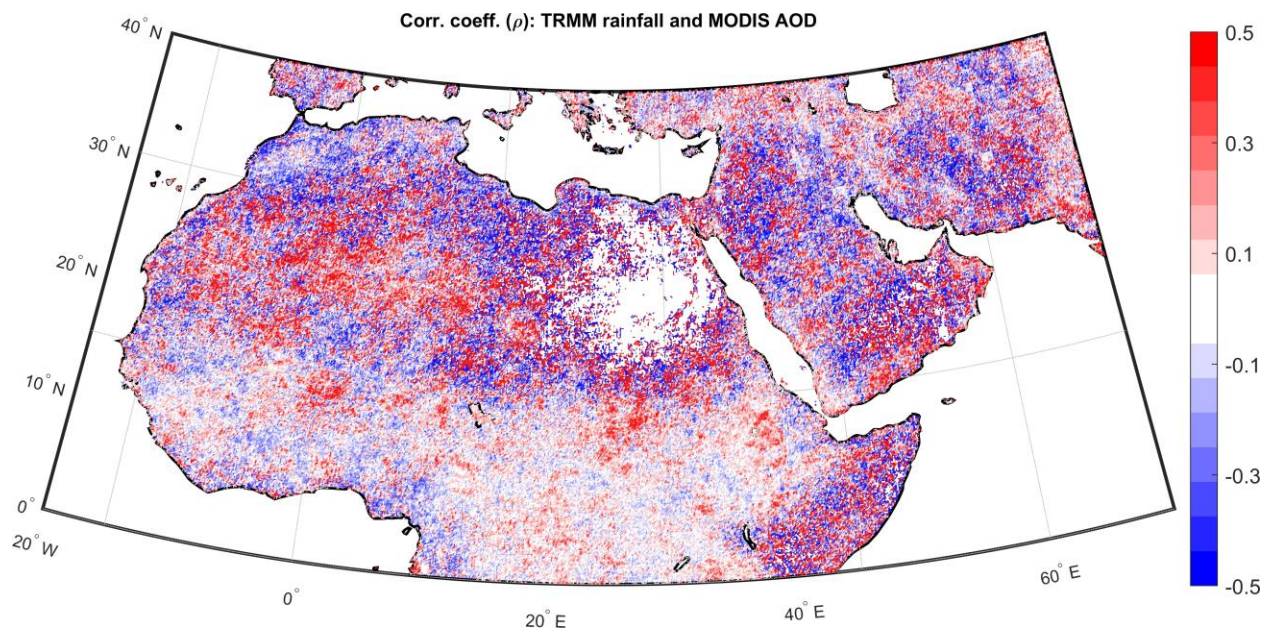
161 In the observational sample, the daily rainfall values vary from zero to 311.8 mm and the AOD  
 162 values range from zero to 3.5 forming a comprehensive sample. The 99<sup>th</sup> percentile of AOD and  
 163 rainfall values are 1.02, and 55.63 (mm), respectively. The histogram of AOD and rainfall are  
 164 shown in Fig. 3.

165 Figure 4 shows the spatial map of correlation coefficient ( $\rho$ ) over the MENA region obtained as  
 166 described in section 2.3. Rainfall is strongly correlated with AOD, some areas showing positive  
 167 correlation and others showing negative correlation. Among the 360,000 (400×900) grid points  
 168 in the map, 30% have positive  $\rho$ , 34.5% have negative  $\rho$  and the rest 35.5% have no data (NaN).  
 169 There is no any identifiable spatial coherence in the grids with positive and negative correlation.



170

171 Figure 3. Histograms of daily MODIS AOD and TRMM rainfall data over the study domain  
 172 (Middle East and North Africa) used for the analysis of dust-rainfall connections.



173

174

175 Figure 4. Spatial map of time correlation coefficient ( $\rho$ ) between MODIS AOD and TRMM  
 176 rainfall derived using daily-mean data for 2015/16.

177 Figure 5 shows the scatter plot between MODIS AOD and TRMM rainfall obtained after  
 178 processing the data as described in section 2.3. Figure 5a and 5b correspond to grids with  
 179 negative and positive correlations, respectively. Among the grids showing negative correlation,  
 180 rainfall decreased exponentially with AOD, which is represented well with an exponential model  
 181 as presented in eq. 1 below.



182 
$$\text{Rainfall} = a \times e^{(b \times \text{AOD})} \tag{1}$$

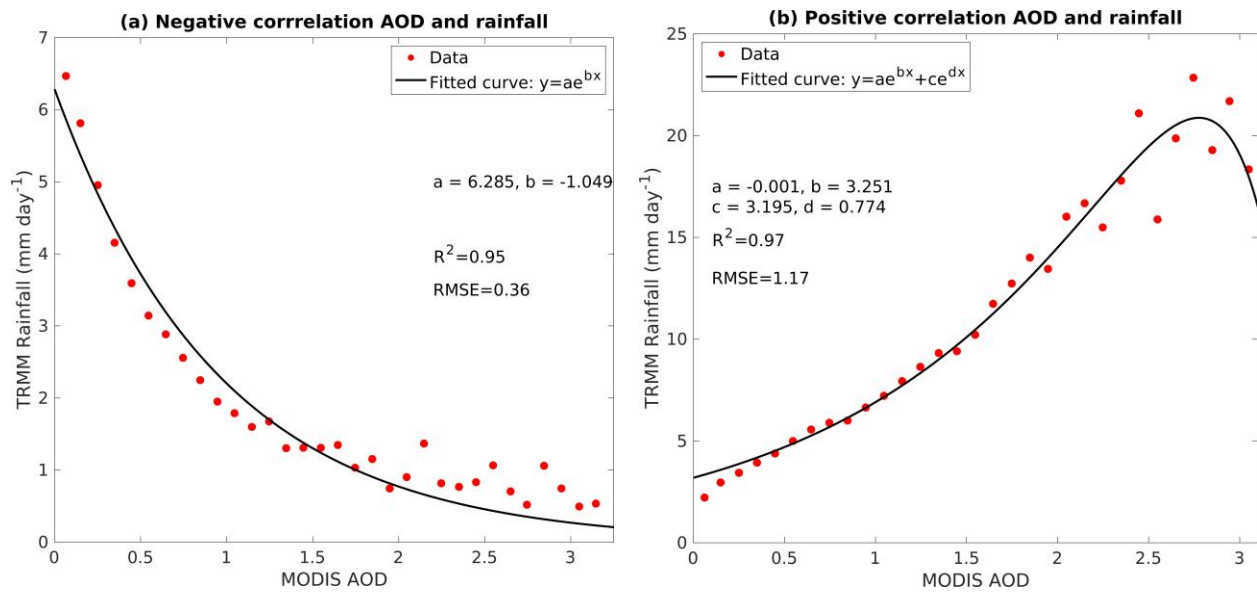
183 Where,  $a = 6.285$  and  $b = -1.049$ .

184 Similarly, among the positively correlated grids, rainfall increased exponentially with AOD,  
 185 which is fitted well by a two-term exponential model as shown in eq. 2 below.

186 
$$\text{Rainfall} = a \times e^{(b \times \text{AOD})} + c \times e^{(d \times \text{AOD})} \tag{2}$$

187 Where,  $a = -0.001$ ,  $b = 3.251$ ,  $c = 3.195$ , and  $d = 0.774$ .

188



189

190 Figure 5. Scatter plot between MODIS AOD and TRMM rainfall obtained following the flow  
 191 chart in Fig. 2 for grids with (a) negative correlations and (b) positive correlations.

192 As seen in Figure 5, AOD values range from 0 to ~ 3 in both cases meaning that the relationships  
 193 represent a diverse environmental conditions possible in nature, from clear to very dusty, with  
 194 the larger values corresponding to large-scale dust storms. One interesting feature of the plots  
 195 worth noting is that the range of rainfall values are very different in the two cases, which  
 196 suggests natural segregation of data in the grids with positive and negative correlations. Negative  
 197 and positive relationship correspond to low ( $0.5 - 6.5 \text{ mm day}^{-1}$ ) and high ( $2 -$   
 198  $22.6 \text{ mm day}^{-1}$ ) rainfall conditions, respectively.

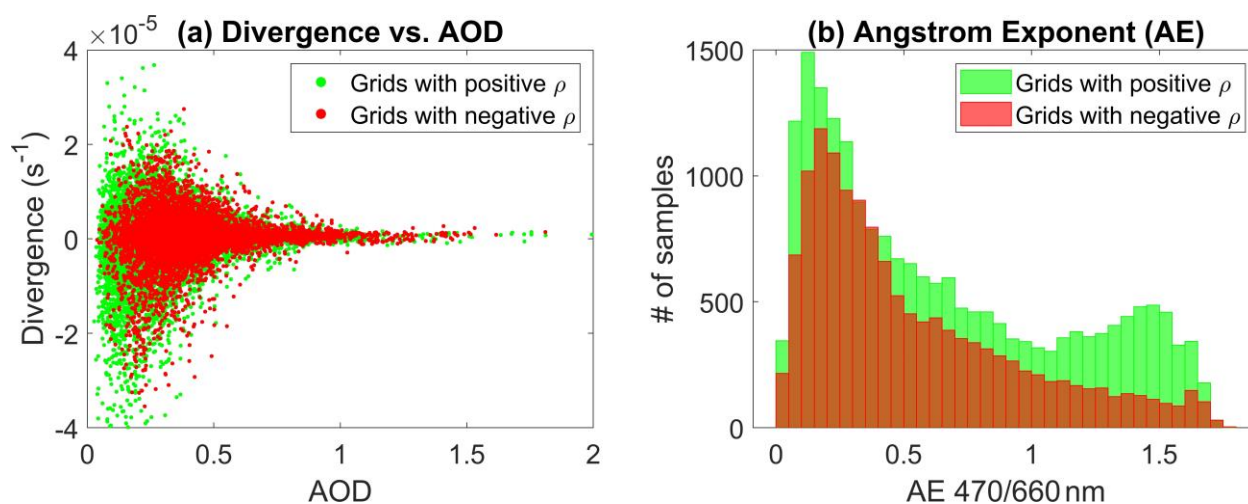
199 The negative correlations could be caused by three possible physical mechanisms. First and most  
 200 likely, it could represent the suppression effect of aerosols on rainfall, which is a known process  
 201 in the areas of deep convection in the early stage through aerosol invigoration (Koren et al.,  
 202 2008; Chakraborty et al., 2018; Fan et al., 2018). Aerosol invigoration is a process in which  
 203 aerosols delay the rainfall in the initial stage of convection but causes more rainfall in the mature  
 204 stage because of the formation of deeper and bigger clouds (Andreae et al., 2004; Koren et al.,  
 205 2005; Koren et al., 2008; Koren et al., 2010; Chakraborty et al., 2018; Fan et al., 2018). Presence

206 of fine aerosol particles in the atmosphere facilitates formation of smaller cloud droplets and  
207 therefore suppress rainfall initially. This suppression allows the cloud droplets to reach the  
208 freezing point as they rise up to higher altitude. Upon freezing, these hydrometeors release more  
209 latent heat, which ultimately intensifies convective updrafts and associated cold rainfall (Koren  
210 et al., 2008; Lee et al., 2012).

211 Second, it could also mean the effect of wet deposition because the rainfall can wash out  
212 aerosols, which decreases the AOD. However, this is unlikely because the negative relationship  
213 is observed in the low-rainfall regime with average rainfall  $< 6$  mm (Fig. 5a), where wet  
214 deposition would be very weak. Lastly, it could happen erroneously when aerosols lie above or  
215 below cloud layers, however, in such cases, a systematic correlation between AOD and rainfall  
216 as observed is unlikely. We note that the Deep blue algorithm has a rigorous cloud-screening  
217 method (Hsu et al., 2013), which effectively masks the cloudy pixels. Such cloud pixels appear  
218 as NaNs in the MODIS AOD data; therefore, our dataset does not represent cloudy conditions.

219 There are also multiple possible causes for the positive relationship. First, it could represent  
220 haboob-type dust events because dust storms and rainfall tend to occur together during these  
221 events (Anisimov et al., 2018). Second, it could also indicate the enhancement effect of aerosols  
222 on rainfall that occur through direct effect of dust on radiation (e.g., elevated heat pump  
223 hypothesis). However, most likely, the positive relationship could mean the indirect effect of  
224 aerosols, i.e., the increased aerosol concentration can contribute to more CCN and thus more  
225 rainfall, which is supported by regional observations as well (e.g., Pósfai et al., 2013). The  
226 observed positive relationship is consistent with a recent study by Choudhury et al., 2020, which  
227 demonstrated the association between high rainfall events with high AOD values using the same  
228 MODIS AOD and TRMM rainfall dataset for multiple years. However, the study did not show  
229 any quantitative connection as we showed (Fig. 5) and the underlying physical mechanism was  
230 not clear, which we explore further in this study.

231



232

233

234 Figure 6. (a) Relationship between divergence and AOD (b) Angstrom Exponent (AE) in grids  
235 with positive and negative correlations between AOD and rainfall.

236 In order to understand the physical mechanism causing positive and negative correlations  
237 between AOD and rainfall, the divergence and AE data are examined.

238 Figure 6a shows the column-averaged divergence at a time closest to MODIS retrievals (12:00  
239 UTC) averaged in time for the analysis period (2015-16), separately for grids with positive and  
240 negative correlations. In the grids with positive correlations, divergence and convergence both  
241 are much stronger than those with negative correlations. Stronger convergence and divergence  
242 both are associated with stronger surface winds, which cause stronger dust mobilization. Higher  
243 negative values represent stronger convergence, which simply means the occurrence of stronger  
244 convection. Since convection is associated with stronger upward motion, the aerosol particles  
245 reach the higher atmosphere. Higher positive values of divergence represents stronger downward  
246 motion, which is possibly related to haboob-type dust events because they are associated with  
247 stronger downdrafts in thunderstorms (Anisimov et al., 2019).

248 Figure 6b shows distribution of average AE calculated for the two cases. There is an interesting  
249 difference in the distribution of AE in positive and negative cases. While the distribution  
250 monotonously decreases towards larger values in the negative case, it starts to increase at  $\sim 1.10$   
251 in the positive case indicating the existence of a peculiar fine-mode component of aerosols. This  
252 indicates that fine-mode aerosol is contributing to the positive relationship between AOD and  
253 rainfall. The existence of fine-mode aerosols suggest that haboob-type dust events are not  
254 contributing to this positive relationship because haboob dust storms are near-surface dust events  
255 which are dominated by coarse-mode dust particles. Similarly, dominance of coarser particles in  
256 the negative case suggest that the negative relationship between AOD and rainfall is governed by  
257 coarse-mode aerosol particles. This analysis indicates that the aerosol indirect effects associated  
258 with convection likely cause the positive and negative relationship between AOD and rainfall.  
259 The negative relationship represent the initial stage of convection because coarser particles are  
260 more abundant in the lower atmosphere which suppress the rain initially as the increase in  
261 particle concentration facilitates formation of more cloud droplets. The positive relationship  
262 represent mature stage of convection, in which the dust particles reaching the higher atmosphere  
263 act as CCN/IN and contribute to cloud development and rainfall formation. In other words, these  
264 results support the idea of aerosol invigoration (e.g., Andreae et al., 2004; Koren et al., 2008;  
265 Chakraborty et al., 2018; Fan et al., 2018).

## 266 *Discussion and Limitations*

267 Although large sample of observational data is used in the analysis, there are some data  
268 limitations. The observed relationship between rainfall and AOD should be broadly considered  
269 as the association between atmospheric aerosols and rainfall, as the AOD represent contribution  
270 from all aerosol types not only dust. Some contamination from other aerosols in the study region  
271 is possible, for example, with biomass burning over the Sahel region (e.g., Bond et al., 2013) and  
272 with sulfate over the Arabian Peninsula (Pósfai et al., 2013; Ukhov et al., 2020; Parajuli et al.,

273 2020). However, such effects are small since dust contributes more than 90% on AOD in the  
274 region (Parajuli et al., 2020).

275 The relationship between aerosol and rainfall is extremely complex particularly because the  
276 clouds are extremely chaotic with very high spatiotemporal variability. In this context, satellite  
277 data can only capture the localized correlations for a given AOD vs rain amount. This study thus  
278 does not fully capture the aerosol-rainfall relationship that is dependent upon the dynamics of  
279 clouds. In addition, the relationship between aerosol and rainfall could be dependent upon  
280 seasons, which should be explored further using longer-term data in future studies. Lastly, both  
281 the AOD and rainfall data are column-average properties, which do not show the distribution of  
282 aerosol concentration and rainfall in the vertical dimension (Parajuli et al., 2020). Therefore, it is  
283 important to look at their vertical distribution to understand the underlying microphysical  
284 processes governing dust-rainfall connections, which should be explored in future studies.  
285 Although the rainfall seems to be clearly associated with AOD in observations, the validity of the  
286 cause-and-effect relationship needs to be examined independently using model simulations.

287 This study has broader social and environmental implications because increased rainfall  
288 contributes to replenishing surface and ground water thus increasing the amount of fresh water  
289 resources in the region (Mostamandi et al., 2020). The results demonstrate a possible physically  
290 based association between dust and rainfall over the MENA region. While dust and dust storms  
291 are generally considered detrimental from an air quality perspective, this study highlights their  
292 positive contribution in making rain, an essential element of plant and animal life.

## 293 **Conclusion**

294 In this work, connection between dust and rainfall is examined using daily-scale satellite  
295 observations. A large data sample from the TRMM rainfall dataset and MODIS AOD dataset are  
296 analyzed for the years of 2015 and 2016 over the MENA region. Using these direct observations,  
297 a quantitative relationship between AOD and rainfall is extracted. Contrasting AOD-rainfall  
298 relationships are observed between high and low rainfall cases under a similar range of AOD  
299 variations. Rainfall decreased (increased) exponentially with AOD in low (high) rainfall cases,  
300 which are represented well with a one-term (two-term) exponential model. The physical basis of  
301 these relationships was explored using divergence and Angstrom Exponent data, which suggest  
302 that the positive (negative) relationship between AOD and rainfall could represent aerosol  
303 indirect effects during the mature (initial) stage of convection.

304

## 305 **Data availability**

306 MODIS AOD data were downloaded from <http://ladsweb.nascom.nasa.gov/data/>. TRMM data  
307 were obtained from the NASA Goddard Earth Sciences Data and Information Services Center  
308 (GES DISC) available at <https://disc.gsfc.nasa.gov/>. ECMWF Operational Analysis data are  
309 restricted data, which were retrieved from [http://apps.ecmwf.int/archive-](http://apps.ecmwf.int/archive-catalogue/?type=4v&class=od&stream=oper&expver=1)  
310 [catalogue/?type=4v&class=od&stream=oper&expver=1](http://apps.ecmwf.int/archive-catalogue/?type=4v&class=od&stream=oper&expver=1) with a membership. A copy of the data  
311 used in the analysis may be obtained by request to the author at [psagar@utexas.edu](mailto:psagar@utexas.edu).

312 **References**

- 313 Andreae, M.O., Rosenfeld, D., Artaxo, P., Costa, A.A., Frank, G.P., Longo, K.M. and Silva-  
314 Dias, M.D.: Smoking rain clouds over the Amazon, *Science*, 303(5662), 1337-1342,  
315 <https://doi.org/10.1126/science.1092779>, 2004.
- 316 Abbott, T. H. and Cronin, T. W.: Aerosol invigoration of atmospheric convection through  
317 increases in humidity, *Science*, 371 (6524), 83-85,  
318 <https://doi.org/10.1126/science.abc5181>, 2021.
- 319 Alizadeh- Choobari, O.: Impact of aerosol number concentration on precipitation under different  
320 precipitation rates. *Meteorological Applications*, 25, 596– 605,  
321 <https://doi.org/10.1002/met.1724>, 2018.
- 322 Ansmann, A., Mattis, I., Müller, D., Wandinger, U., Radlach, M., Althausen, D., et al.: Ice  
323 formation in Saharan dust over central Europe observed with  
324 temperature/humidity/aerosol Raman lidar, *Journal of Geophysical Research*, 110,  
325 D18S12, <https://doi.org/10.1029/2004jd005000>, 2005.
- 326 Anisimov, A., Tao, W., Stenchikov, G., Kalenderski, S., Prakash, P. J., Yang, Z.-L., and Shi, M.:  
327 Quantifying local-scale dust emission from the Arabian Red Sea coastal plain,  
328 *Atmospheric Chemistry and Physics*, 17, 993–1015, [https://doi.org/10.5194/acp-17-993-](https://doi.org/10.5194/acp-17-993-2017)  
329 [2017](https://doi.org/10.5194/acp-17-993-2017), 2017.
- 330 Bond, T. C., et al.: Bounding the role of black carbon in the climate system: A scientific  
331 assessment, *Journal of Geophysical Research*, 118(11), 5380–5552,  
332 <https://doi.org/10.1002/jgrd.50171>, 2013.
- 333 Chakraborty, S., Fu, R., Rosenfeld, D., & Massie, S. T.: The influence of aerosols and  
334 meteorological conditions on the total rain volume of the mesoscale convective systems  
335 over tropical continents, *Geophysical Research Letters*, 45, 13,099– 13,106.  
336 <https://doi.org/10.1029/2018GL080371>, 2018.
- 337 Choudhury, G., Tyagi, B., Vissa, N. K., Singh, J., Sarangi, C., Tripathi, S. N., and Tesche, M.:  
338 Aerosol-enhanced high precipitation events near the Himalayan foothills, *Atmospheric*  
339 *Chemistry and Physics*, 20, 15389–15399, [https://doi.org/10.5194/acp-20-15389-](https://doi.org/10.5194/acp-20-15389-2020)  
340 [2020](https://doi.org/10.5194/acp-20-15389-2020).
- 341 Creamean, J. M., Suski, K. J., Rosenfeld, D., Cazorla, A., DeMott, P. J., Sullivan, R. C., et al.:  
342 Dust and biological aerosols from the Sahara and Asia influence precipitation in the  
343 Western U.S, *Science*, 339(6127), 1572–1578, <https://doi.org/10.1126/science.1227279>,  
344 2013.
- 345 Dennis, A.S.: Weather modification by cloud seeding, *International geophysics series*, 24, 670,  
346 [https://digitalcommons.usu.edu/water\\_rep/670](https://digitalcommons.usu.edu/water_rep/670), 1980.
- 347 Eck, T. F., et al.: Spatial and temporal variability of column- integrated aerosol optical  
348 properties in the southern Arabian Gulf and United Arab Emirates in summer, *Journal of*  
349 *Geophysical Research*, 113, D01204, <https://doi.org/10.1029/2007JD008944>, 2008.
- 350 Fan, J., Rosenfeld, D., Zhang, Y., Giangrande, S.E., Li, Z., Machado, L.A., Martin, S.T., Yang,  
351 Y., Wang, J., Artaxo, P. and Barbosa, H.M.: Substantial convection and precipitation  
352 enhancements by ultrafine aerosol particles, *Science*, 359 (6374), 411-418,  
353 <https://doi.org/10.1126/science.aan8461>, 2018.
- 354 Grabowski, W. W., and Morrison, H.: Do Ultrafine Cloud Condensation Nuclei Invigorate Deep  
355 Convection?, *Journal of the Atmospheric Sciences*, 77(7), 2567-2583,  
356 <https://doi.org/10.1175/JAS-D-20-0012.1>, 2020.

357 Han, Y., Fang, X., Zhao, T., Bai, H., Kang, S., and Song, L.: Suppression of precipitation by dust  
358 particles originated in the Tibetan Plateau, *Atmospheric Environment*, 43(3), 568-574,  
359 <https://doi.org/10.1016/j.atmosenv.2008.10.018>, 2009.

360 Huffman, G.J., D.T. Bolvin, E.J. Nelkin, and R.F. Adler (2016), TRMM (TMPA) Precipitation  
361 L3 1 day 0.25 degree x 0.25 degree V7, Edited by Andrey Savtchenko, Goddard Earth  
362 Sciences Data and Information Services Center (GES DISC), Accessed: [January 22,  
363 2022], 10.5067/TRMM/TMPA/DAY/7.

364 Jacobson, M. Z. and Kaufman, Y. J.: Wind reduction by aerosol particles, *Geophysical Research*  
365 *Letters*, 33, L24814, <https://doi.org/10.1029/2006GL027838>, 2006.

366 Jin, Q., Wei, J., Yang, Z.-L., Pu, B., and Huang, J.: Consistent response of Indian summer  
367 monsoon to Middle East dust in observations and simulations, *Atmos. Chem. Phys.*, 15,  
368 9897–9915, <https://doi.org/10.5194/acp-15-9897-2015>, 2015.

369 Konare, A., Zakey, A. S., Solmon, F., Giorgi, F., Rauscher, S., Ibrah, S., et al.: A regional  
370 climate modeling study of the effect of desert dust on the West African monsoon, *Journal*  
371 *of Geophysical Research*, 113, D12206, <https://doi.org/10.1029/2007JD009322>, 2008.

372 Koren, I., Kaufman, Y. J., Rosenfeld, D., Remer, L. A., and Rudich, Y.: Aerosol invigoration  
373 and restructuring of Atlantic convective clouds, *Geophysical Research Letters*, 32,  
374 L14828, <https://doi.org/10.1029/2005GL023187>, 2005.

375 Koren, I., Martins, J.V., Remer, L.A. and Afargan, H.: Smoke invigoration versus inhibition of  
376 clouds over the Amazon, *Science*, 321(5891), 946-949,  
377 <https://doi.org/10.1126/science.1159185>, 2008.

378 Lau, W. K. M., Kim, M.-K., Kim, K.-M. and Lee, W.-S.: Enhanced surface warming and  
379 accelerated snow melt in the Himalayas and Tibetan Plateau induced by absorbing  
380 aerosols, *Environmental Research Letters*, 5, 025204, [https://doi.org/10.1088/1748-](https://doi.org/10.1088/1748-9326/5/2/025204)  
381 [9326/5/2/025204](https://doi.org/10.1088/1748-9326/5/2/025204), 2010.

382 Lee, S.S.: Effect of Aerosol on Circulations and Precipitation in Deep Convective Clouds.  
383 *Journal of Atmospheric Science*, 69, 1957–1974, [https://doi.org/10.1175/JAS-D-11-](https://doi.org/10.1175/JAS-D-11-0111.1)  
384 [0111.1](https://doi.org/10.1175/JAS-D-11-0111.1), 2012.

385 Li, R., Min, Q. and Harrison, L. C.: A Case Study: The Indirect Aerosol Effects of Mineral Dust  
386 on Warm Clouds, *Journal of Atmospheric Science*, 67, 805–  
387 816, <https://doi.org/10.1175/2009JAS3235.1>, 2010.

388 Li, Z., Niu, F., Fan, J., Liu, Y., Rosenfeld, D. and Ding, Y.: Long-term impacts of aerosols on the  
389 vertical development of clouds and precipitation, *Nature Geoscience*, 4(12), 888-894,  
390 <https://doi.org/10.1038/ngeo1313>, 2011.

391 Liu, Z., Ostrenga, D., Teng, W. and Kempler, S.: Tropical Rainfall Measuring Mission (TRMM)  
392 Precipitation Data and Services for Research and Applications, *Bulletin of American*  
393 *Meteorological Society*, 93, 1317–1325, <https://doi.org/10.1175/BAMS-D-11-00152.1>,  
394 [2012](https://doi.org/10.1175/BAMS-D-11-00152.1).

395 Lohmann, U. and Feichter, J.: Can the direct and semi- direct aerosol effect compete with the  
396 indirect effect on a global scale?, *Geophysical Research Letters*, 28(1), 159-161,  
397 <https://doi.org/10.1029/2000GL012051>, 2001.

398 Parajuli, S. P., Stenchikov, G. L., Ukhov, A., & Kim, H.: Dust emission modeling using a new  
399 high-resolution dust source function in WRF-Chem with implications for air quality.  
400 *Journal of Geophysical Research: Atmospheres*, 124, 10109– 10133.  
401 <https://doi.org/10.1029/2019JD030248>, 2019.



402 Parajuli, S. P., Stenchikov, G. L., Ukhov, A., Shevchenko, I., Dubovik, O., and Lopatin, A.:  
403 Aerosol vertical distribution and interactions with land/sea breezes over the eastern coast  
404 of the Red Sea from lidar data and high-resolution WRF-Chem simulations, *Atmos.*  
405 *Chem. Phys.*, 20, 16089–16116, <https://doi.org/10.5194/acp-20-16089-2020>, 2020.

406 Rémy, S., Benedetti, A., Bozzo, A., Haiden, T., Jones, L., Razinger, M., et al.: Feedbacks of dust  
407 and boundary layer meteorology during a dust storm in the eastern Mediterranean,  
408 *Atmospheric Chemistry and Physics*, 15, 12909–12933, [https://doi.org/10.5194/acp-15-](https://doi.org/10.5194/acp-15-12909-2015)  
409 [12909-2015](https://doi.org/10.5194/acp-15-12909-2015), 2015.

410 Stull, R. (2000). *Meteorology for scientists and engineers*. Brooks/Cole, 2000.

411 Sayer, A. M., Hsu, N. C., Bettenhausen, C., and Jeong, M.-J.: Validation and uncertainty  
412 estimates for MODIS Collection 6 “Deep Blue” aerosol data, *J. Geophys. Res. Atmos.*,  
413 118, 7864–7872, <https://doi.org/10.1002/jgrd.50600>, 2013.

414 Sayer, A. M., Hsu, N. C., Lee, J., Kim, W. V., & Dutcher, S. T.: Validation, stability, and  
415 consistency of MODIS collection 6.1 and VIIRS version 1 Deep Blue aerosol data over  
416 land, *Journal of Geophysical Research: Atmospheres*, 124, 4658–4688,  
417 <https://doi.org/10.1029/2018JD029598>, 2019.

418 Twohy, C.H.: Measurements of Saharan Dust in Convective Clouds over the Tropical Eastern  
419 Atlantic Ocean, *Journal of Atmospheric Science*, 72, 75–81, [https://doi.org/10.1175/JAS-](https://doi.org/10.1175/JAS-D-14-0133.1)  
420 [D-14-0133.1](https://doi.org/10.1175/JAS-D-14-0133.1), 2015.

421 Ukhov, A., Mostamandi, S., da Silva, A., Flemming, J., Alshehri, Y., Shevchenko, I., and  
422 Stenchikov, G.: Assessment of natural and anthropogenic aerosol air pollution in the  
423 Middle East using MERRA-2, CAMS data assimilation products, and high-resolution  
424 WRF-Chem model simulations, *Atmospheric Chemistry and Physics*, 20, 9281–9310,  
425 <https://doi.org/10.5194/acp-20-9281-2020>, 2020.